



OPEN ACCESS

EDITED BY

Kamen Atanasov Tsvetanov,
University of Cambridge, United Kingdom

REVIEWED BY

Jiaying Lu,
Fudan University, China
Min Wang,
Shanghai University, China
Sudeepti Southekal,
Eli Lilly and Company, United States

*CORRESPONDENCE

Hillary Protas
✉ hillary.protas@bannerhealth.com

SPECIALTY SECTION

This article was submitted to
Brain Imaging Methods,
a section of the journal
Frontiers in Neuroscience

RECEIVED 03 November 2022

ACCEPTED 14 February 2023

PUBLISHED 02 March 2023

CITATION

Protas H, Ghisays V, Goradia DD, Bauer R III,
Devadas V, Chen K, Reiman EM and Su Y
(2023) Individualized network analysis: A novel
approach to investigate tau PET using graph
theory in the Alzheimer's disease continuum.
Front. Neurosci. 17:1089134.
doi: 10.3389/fnins.2023.1089134

COPYRIGHT

© 2023 Protas, Ghisays, Goradia, Bauer,
Devadas, Chen, Reiman and Su. This is an
open-access article distributed under the terms
of the [Creative Commons Attribution License
\(CC BY\)](#). The use, distribution or reproduction
in other forums is permitted, provided the
original author(s) and the copyright owner(s)
are credited and that the original publication in
this journal is cited, in accordance with
accepted academic practice. No use,
distribution or reproduction is permitted which
does not comply with these terms.

Individualized network analysis: A novel approach to investigate tau PET using graph theory in the Alzheimer's disease continuum

Hillary Protas^{1,2*}, Valentina Ghisays^{1,2}, Dhruvan D. Goradia^{1,2},
Robert Bauer III^{1,2}, Vivek Devadas^{1,2}, Kewei Chen^{1,2,3,4,5},
Eric M. Reiman^{1,2,3,4,5,6} and Yi Su^{1,2,5} for the Alzheimer's
Disease Neuroimaging Initiative

¹Banner Alzheimer's Institute, Phoenix, AZ, United States, ²Arizona Alzheimer's Consortium, Phoenix, AZ, United States, ³Department of Neurology, The University of Arizona, Tucson, AZ, United States, ⁴Department of Psychiatry, The University of Arizona, Tucson, AZ, United States, ⁵Department of Neuroscience, School of Computing and Augmented Intelligence, Biostatistical Core, School of Mathematics and Statistics, College of Health Solutions, Arizona State University, Tempe, AZ, United States, ⁶Translational Genomics Research Institute, Phoenix, AZ, United States

Introduction: Tau PET imaging has emerged as an important tool to detect and monitor tangle burden in vivo in the study of Alzheimer's disease (AD). Previous studies demonstrated the association of tau burden with cognitive decline in probable AD cohorts. This study introduces a novel approach to analyze tau PET data by constructing individualized tau network structure and deriving its graph theory-based measures. We hypothesize that the network-based measures are a measure of the total tau load and the stage through disease.

Methods: Using tau PET data from the AD Neuroimaging Initiative from 369 participants, we determine the network measures, global efficiency, global strength, and limbic strength, and compare with two regional measures entorhinal and tau composite SUVR, in the ability to differentiate, cognitively unimpaired (CU), MCI and AD. We also investigate the correlation of these network and regional measures and a measure of memory performance, auditory verbal learning test for long-term recall memory (AVLT-LTM). Finally, we determine the stages based on global efficiency and limbic strength using conditional inference trees and compare with Braak staging.

Results: We demonstrate that the derived network measures are able to differentiate three clinical stages of AD, CU, MCI, and AD. We also demonstrate that these network measures are strongly correlated with memory performance overall. Unlike regional tau measurements, the tau network measures were significantly associated with AVLT-LTM even in cognitively unimpaired individuals. Stages determined from global efficiency and limbic strength, visually resembled Braak staging.

Discussion: The strong correlations with memory particularly in CU suggest the proposed technique may be used to characterize subtle early tau accumulation. Further investigation is ongoing to examine this technique in a longitudinal setting.

KEYWORDS

flortaucipir PET, graph theory, Alzheimer's disease, tangle burden, ADNI

1. Introduction

Both Amyloid and tau begin building up long before clinical symptoms of Alzheimer's disease (Jack et al., 2010, 2017b). Characterizing the level of tau pathology and its progression is of vital importance. Braak staging describes the spatial pattern of tau pathology and its spread from entorhinal and limbic to isocortical regions based on neuropathological studies (Braak and Braak, 1991, 1995). With the advent of tau PET tracers it is possible to measure the distribution of tangle burden *in vivo* and characterize its progression over time (Chien et al., 2013; Dani et al., 2016; Schwarz et al., 2018). Braak regions have been defined by FreeSurfer regions and conditional inference tree regression model (Scholl et al., 2016; Maass et al., 2017). Other *in vivo* Braak strategies have been adopted as well Schwarz et al. (2016, 2018). A meta-temporal region of interest which is defined as a collection of Braak III-IV regions has been proposed as a global index of overall tau burden (Jack et al., 2017a,b). While the spatial distribution of tau pathology generally follows the Braak stages, individual variability exists in where tau starts in the cortex and how it progresses (Braak et al., 2011; Franzmeier et al., 2020; Sanchez et al., 2021; Vogel et al., 2021). An alternative strategy to analyze tau PET data would still investigate tau spread throughout the brain in disease but allows for variability in the spatial pattern of tangle burden and does not necessarily follow Braak staging.

Graph-based or network approach can provide such an alternative and has been shown to allow detection of subtle changes of the brain antecede well known Alzheimer's disease (AD) deficits (Morris et al., 2001; Albert, 2011; Arlt et al., 2013) without defined staging. This approach has been widely adopted to characterize the blood oxygen level dependent (BOLD) signal in resting state fMRI images for the investigation of brain function in health and disease (Wang et al., 2010, 2011; Braun et al., 2012; Hojjati et al., 2019). With this approach, a complex network can be constructed with nodes representing regional measures and edges describing relationship between nodes. Network-based measurements can then be used to identify modular structure in these networks (Wang et al., 2010, 2011; Farahani et al., 2019). In addition to its numerous applications in analyzing fMRI data, this approach has been reported for its use in analyzing T1w-MRI and PET data (He et al., 2007, 2008; Huang et al., 2010; Sepulcre et al., 2013, 2018; Tijms et al., 2013, 2018; Wang et al., 2016, 2020; Arnemann et al., 2018; Pereira et al., 2018; Veronese et al., 2019; Kim et al., 2021). Individualized network analyses are already available and very well established particularly in resting state fMRI and Diffusion Tensor Imaging (DTI) (Fornito et al., 2010; Braun et al., 2012; Hojjati et al., 2019). There are a few studies with T1-wMRI and FDG PET where individualized networks have been introduced (Tijms et al., 2012, 2013; Wang et al., 2016, 2020). The weights of both of these past individualized networks and group-based networks are defined by correlation, covariance, or other measures of similarity and association. The weights in new individualized tau networks introduced in this paper are instead characterized by difference in regional tau burden.

In this work, we propose a different approach to construct individual level tau PET networks drawing inspiration from and analogy to the application of graph-theoretical approach in the context of population genetics (Dyer and Nason, 2004; Dyer

et al., 2010; Rodger et al., 2018; Savary et al., 2021a,b). The goal of analyzing tau PET data is to quantify tangle burden across different brain regions and make inference about how tangle burden would progress in a patient. Similarly in population genetics, researchers seek to characterize and quantify genetic variabilities in the overall population and describe genetic flow among different subpopulations using network -based approach for over 15 years (Dyer and Nason, 2004; Rodger et al., 2018; Savary et al., 2021a,b). In these research, a population graph or network, **Figure 1A** for an example, is constructed with each node representing a subpopulation and each edge connecting two nodes characterized by a distance measure representing the genetic difference between the two nodes (Excoffier et al., 1992; Dyer and Nason, 2004; Garroway et al., 2008; Dyer, 2009; Dyer et al., 2010; Manel and Holderegger, 2013; Shirk et al., 2018; Savary et al., 2021b). Therefore, similar to the application of graph-theoretical approach in population genetics research, we propose to construct individual level tau PET networks with each node representing different anatomical regions and the edge between the two nodes characterizing the difference in tau burden and then we derive graph-based metrics from the tau PET networks (**Figure 1B**). We examined the graph-based metrics and their ability to distinguish between cognitively unimpaired (CU), mild cognitive impairment (MCI) and AD participants in comparison to conventional regional analysis. In addition, we also examined the association of each individualized tau network measure with memory performance. We visually compare staging developed from the graph theory measures to Braak staging.

2. Materials and methods

2.1. Study participants

Data used in this study were obtained from participants in the Alzheimer's Disease Neuroimaging Initiative (ADNI) database. Flortaucipir (FTP) PET scans were downloaded as of 11/29/2018 for 32 AD, 115 MCI and 223 CU older adults (**Table 1**). We included all participants with FTP scans from ADNI that also have a matching T1w MRI near the time of the FTP acquisitions (0.3 ± 0.6 years) regardless of the diagnostic status to allow us to examine tau pathology throughout the full AD continuum from biomarker negative cognitively normal participants to clinical AD. Matching T1w MRI and florbetapir (FBP) PET were also downloaded where available. This included participants with preclinical AD defined as those who were cognitively normal but had a positive AD biomarker, e.g., amyloid positive. Participants who did not fit into the typical AD/preclinical AD profile under the ATN framework (Jack et al., 2018) were also included. ADNI study was approved by the institutional review boards of the participating institutions. Signed informed written consent was obtained from each participant. For this project the most fully preprocessed PET images were downloaded from ADNI. The PET images underwent a procedure of between frame motion correction, averaging of the frames, reoriented to standard grid, and finally scanner harmonization filtering to 8 mm at University of Michigan. Details about the scan acquisition for MRI and PET are provided

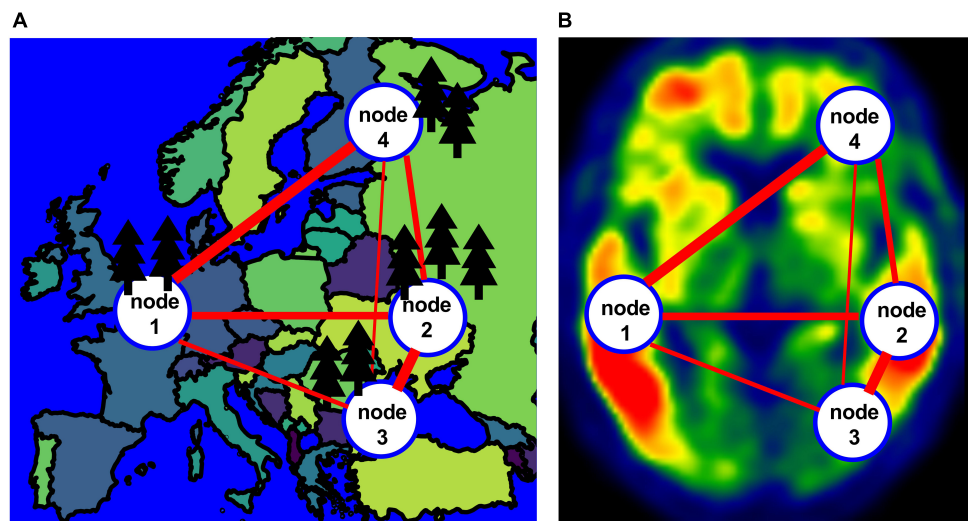


FIGURE 1 (A) An example of a population network with four nodes. (B) An example of the network for a tau image.

TABLE 1 Subject characteristics age, gender, APOE, education, cognitive measures as well as Aβ and tau positivity are included for the three groups (CU, MCI, and AD).

	CU (n = 222)	MCI (n = 115)	AD (n = 32)	p-value
Age	74.5 ± 7.4	76.9 ± 7.2	77.6 ± 9.4	0.003
Gender(M/F)	92/130	73/42	17/15	5e-4
APOE(NC/Car)	137/75	77/37	16/13	0.46
Education	16.7 ± 2.4	16.3 ± 2.7	15.4 ± 2.4	0.01
MMSE***	29.0 ± 1.3	27.8 ± 2.1	21.2 ± 4.8	4e-58
AVLT-LTM	10.0 ± 2.9	4.0 ± 4.0	0.9 ± 2.1	8e-51
AVLT-TL	46.6 ± 10.5	35.3 ± 10.4	22.2 ± 7.8	4e-35
CDR-SB	0.1 ± 0.3	1.2 ± 1.1	6.3 ± 3.1	9e-90
Aβ positivity(pos/neg) * (threshold: 1.17)	50/165	49/63	24/5	1e-10
Tau positivity(pos/neg)** (threshold:1.23)	104/118	80/35	27/5	2e-6

*Aβ positivity is defined by mean cortical region to/cerebellar region with a threshold for positivity of 1.17. **Tau positivity was defined based on the tau composite-SUVr greater than 1.23. ***CDR SB, clinical dementia rating sum of boxes; AVLT-TL, auditory verbal learning test total score, AVLT-LTM, auditory verbal learning test long term memory recall; MMSE, mini mental state examination.

at the ADNI website.¹ In addition to imaging data, demographic, clinical, and cognitive scores including auditory verbal learning test long term memory (AVLT-LTM) scores, Clinical Dementia Rating Scale-Sum of Boxes (CDR-SB), Mini Mental State examination (MMSE) score matching the imaging data were also downloaded from ADNI.

2.2. Image analysis

The FTP image was co-registered to the nearest T1w MRI using SPM12 (Wellcome Trust Centre for Neuroimaging)² and then SPM12 was used to warp MRI and the co-registered FTP image

into Montreal Neurological Institute (MNI) template space. An in-house developed procedure was used to calculate the FTP standard uptake ratio (SUVr) values in template space for an entorhinal region (Braak et al., 2006; Johnson et al., 2016) and a tau composite-SUVr (Jack et al., 2017a,b). The entorhinal region is defined by the Mayo Clinic Adult Lifespan Template (MCALT) with a cerebral crus 1 reference region from Automated Anatomical Labeling (AAL) atlas (Tzourio-Mazoyer et al., 2002). The tau composite was computed as the median-uptake of voxels in entorhinal, amygdala, parahippocampal, fusiform, inferior temporal, and middle temporal regions normalized to cerebellar-crus following the previously described procedure (Jack et al., 2017a,b). This allowed us to determine Tau positivity, defined based on the tau composite-SUVr greater than 1.23 (Jack et al., 2017b). For those participants with a matching FBP scans, the FBP images were warped to the MNI template, amyloid burden was also determined using established methods and positivity is defined by

1 www.adni-info.org

2 <http://www.fil.ion.ucl.ac.uk/spm/>

having a mean cortical to cerebellum SUVR > 1.17 (Fleisher et al., 2011).

2.3. Individual-network based method

A schematic of the method can be seen in Figure 2. The input to the pipeline is the warped tau SUVR image seen in 2A. A probabilistic gray matter mask (binarized with a threshold of 0.3) was used to define valid nodes of the network. For each of the 90 AAL regions (Tzourio-Mazoyer et al., 2002), a six-mm cube at its center (Xia et al., 2013; Yu et al., 2013) was subdivided into a $3 \times 3 \times 3$ matrix with 2-mm isotropic elements as seen in Figure 2B. To be included in the network analysis, such cube must be a) independent of each other (no overlaps) and b) each of the 27 elements has a nonzero gray matter mask value. This left 64 regions (nodes) out of the 90 AAL regions (Supplementary Table 1).

To represent the tau network structure for each individual, an undirected network was constructed by calculating the weight (w) between each pair of nodes using a predefined weighting function. The weighting function is defined as the difference of the means of the two nodes:

$$w_{ij} = |\bar{x}_i - \bar{x}_j| \quad (1)$$

Higher weight indicates a greater difference in tau deposition between the two nodes and vice versa. The inverse of the weight between two nodes defines the network distance. A larger tau interregional distance or weight corresponds with a shorter network distance. The shortest path length (d_{ij}) is defined as minimum network distance between node i and j by either a direct or indirect route. For example, if $d_{ij} > d_{ik} + d_{kj}$ then d_{ij} is set to $d_{ik} + d_{kj}$. In this case, the indirect path is the shorter path and replaces the direct path. The brain connectivity toolbox (BCT)³ (Rubinov and Sporns, 2010) was used to calculate efficiency, strength, and other measures of the network. Our method uses the weighted undirected network instead of binarized network to capitalize on the information carried by the weights.

Two types of network measures that are commonly used in network analysis are examined in this study and briefly summarized here.

2.3.1. Network strength

The network strength of a node (nodal network strength) is defined as the sum of all the weights connected to a node:

$$s_i = \sum_{j \in N} w_{ij} \quad (2)$$

s_i Represents the strength of node i . Average nodal network strength of predefined sets of nodes can be calculated as a local or global measure. A local limbic strength is defined as the mean strength over four nodes (bilateral amygdala and parahippocampal gyrus) within the limbic network well-known to subject to tau pathology in AD (shown in Figure 2D). We use limbic strength as a representative network strength measure in the rest of the analysis to compare with conventional and other network-based tau measurements. A global strength defined as the mean nodal

strength over all nodes is also examined as an overall strength measure of the network.

2.3.2. Network efficiency

In a weighted network, global efficiency (E^w) is a measure of the overall efficiency of information flow through nodes in the network (Eq. 3). It is the average of the inverse of the shortest path lengths. This is the new interregional distance matrix (\tilde{w}_{ij}) that includes both direct and indirect paths. \tilde{w}_{ij} is inversely related to the shortest path length d_{ij} in the network, thus, a shorter path means higher efficiency. This measurement is very similar to network strength.

$$E^w = \frac{1}{n} \sum_{i \in N} \frac{\sum_{j \in N, j \neq i} (d_{ij}^w)^{-1}}{n-1} = \frac{1}{n} \sum_{i \in N} \frac{\sum_{j \in N, j \neq i} \tilde{w}_{ij}}{n-1} \quad (3)$$

From these two types of network measures (strength and efficiency), in this study we focus on three measurements including global strength, limbic strength, and global efficiency.

2.4. Statistical analysis

To assess the utility and relevance of the three tau network measurements (global strength, limbic strength, and global efficiency), statistical analysis was performed to evaluate (1) the ability of these measurements in differentiating CU, MCI and AD groups and (2) the relationship between tau network measurements with cognitive measures. To evaluate the ability to differentiate CU, MCI and AD, Cohen's f effect sizes, and confidence intervals were calculated for ANCOVA analysis for the three groups (CU, MCI, AD) with age and gender as a covariate using "effectsize" library in R. To characterize relationship of tau measures with AVLT-LTM scores (auditory verbal learning test for long-term recall memory), Spearman rank correlation were determined using R version 3.6.1 in CU and combined full groups. For the association analysis of Tau PET measures with memory in the CU group, we excluded participants who had a AVLT-LTM score of less than 5 (Ivnik et al., 1992). A Steiger test was used to compare the correlations for tau measures versus memory within groups using "cocor" library in R. Additional analysis was also performed to investigate the ability of using tau network measures for definition of pathological stages. The ctree function from the "partykit" library in R 3.6.1 was used to classify subjects using conditional inference tree based on the three tau network measures. After determining the stage, we averaged all tau PET images to create an average tau PET for each stage as well as averaging the tau strength for each node. We then created a surface display BrainNet with the nodes with average nodal strength as the size of the node.

3. Results

3.1. Participant characteristics

Demographic characteristics, MMSE, and AVLT-LTM scores are shown in Table 1. Age, education, and gender as well as cognitive and memory scores are significantly different between AD, MCI and CU groups ($p < 0.05$). The proportions of APOE

³ <http://www.brain-connectivity-toolbox.net/>

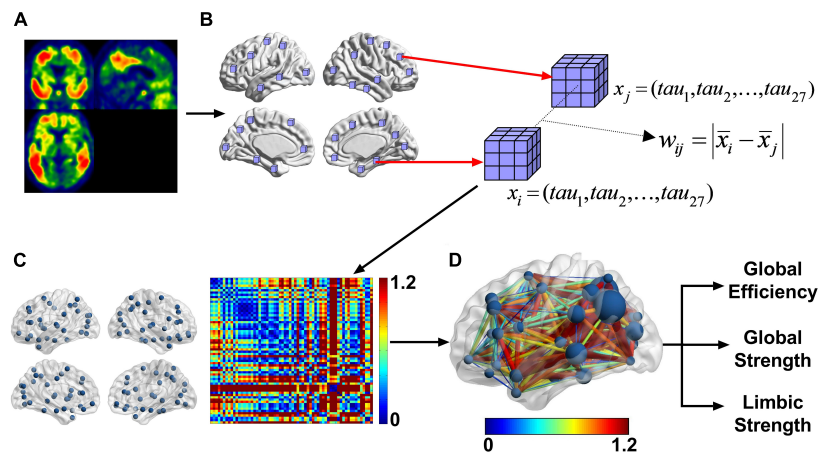


FIGURE 2

After preprocessing the PET images (A) into template space, we took 6 mm × 6 mm × 6 mm cubes centered at each of the AAL regions (B). From that we calculated the difference between the mean tau SUVR of each cube. This resultant matrix is shown as a heatmap (C). This is a weighted undirected network. The image in panel (D) is another representation of the weighted undirected matrix with the graph on the brain and the color representing the difference of regional tau SUVR. The size of the node is the strength. Each subject in this cross-sectional study had a graph for FTP and from that graph the global strength, global efficiency, and limbic strength can be calculated. Limbic strength is the strength over the bilateral parahippocampal and amygdala nodes.

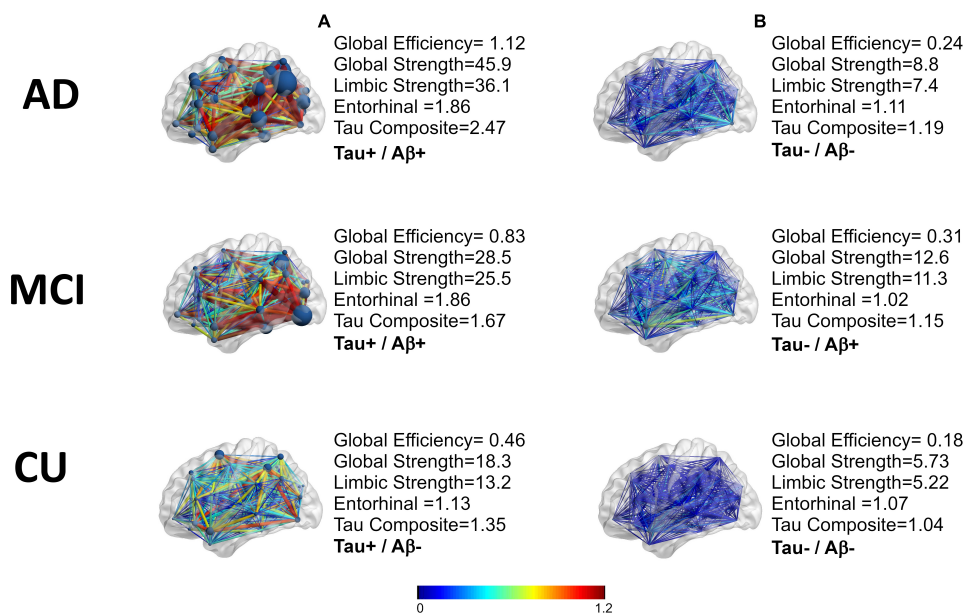


FIGURE 3

A representation of the tau networks for two subjects from each of the three clinical groups (AD, MCI, CU). The difference of the means of the weights are in color. The nodal strength can be seen as the size of the nodes. Tau positivity was defined based on the tau composite-SUVR greater than 1.23, (A) are tau positive and (B) are tau negative. Aβ positivity is defined by mean cortical region to/cerebellar region with a threshold for positivity of 1.17.

carriers were not significantly different between the three groups ($p = 0.46$).

3.2. Tau network characteristics

An example of the distance matrices of undirected networks derived from FTP images can be seen in Figure 2C. The tau networks are also displayed using BrainNet viewer (Xia et al., 2013)

with the color representing the weights of the network and size of the nodes representing strength (Figures 2D, 3). Tau networks for a tau positive (left) and a tau negative (right) subject were randomly chosen from each of the clinical groups (i.e., CU, MCI, and AD) for illustration (Figure 3). Measurements for global efficiency, global strength, and limbic strength as well as the tau composite SUVR, entorhinal tau SUVR were also listed in Figure 3 for each selected subject. There is a general trend for AD patients than MCI and CU to have higher between-node distances. But it is not

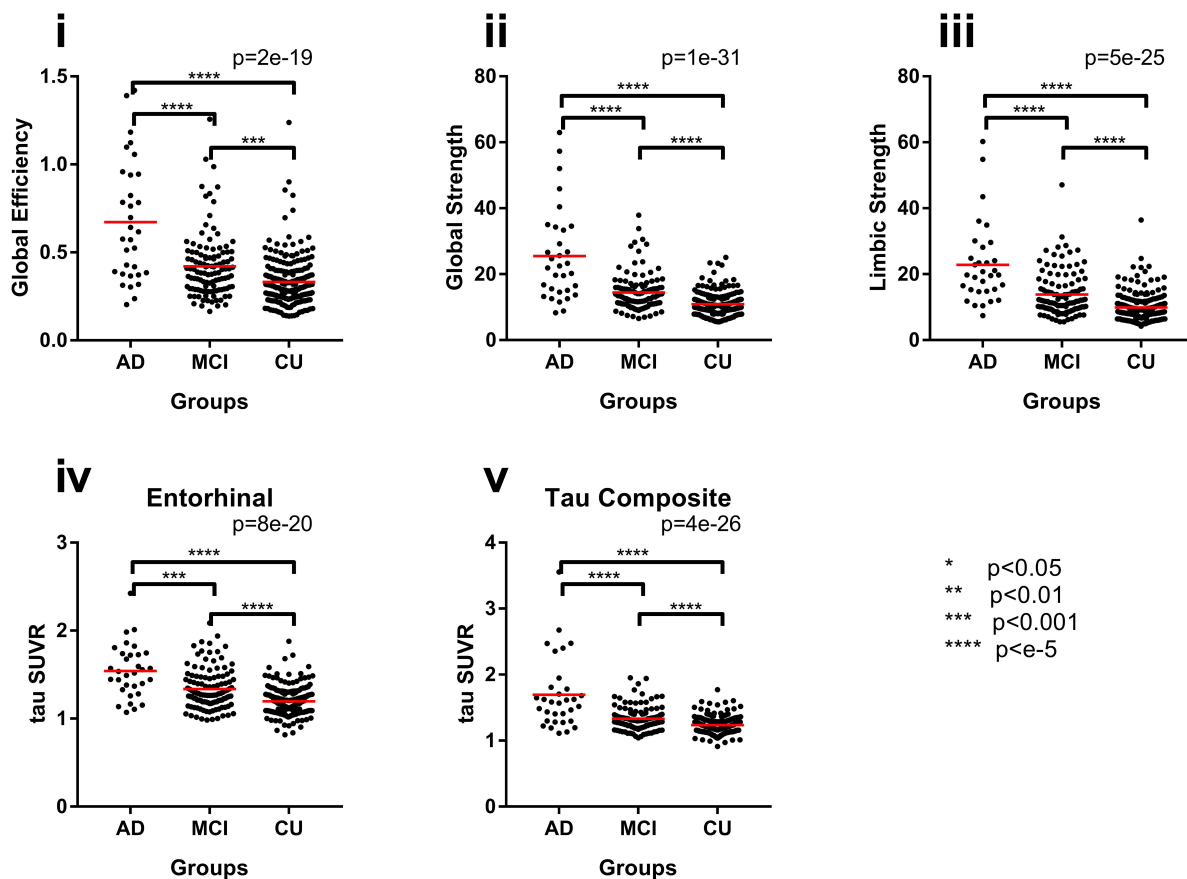


FIGURE 4

Group differences with network measures for the original FTP networks, (i) global efficiency, (ii) global strength, and (iii) limbic strength, and common regional measures, (iv) entorhinal SUVR and (v) tau composite SUVR between AD, MCI, and CU subjects. * $p < 0.05$, ** $p < 0.01$, *** $p < 0.001$, **** $p < e-5$.

recommended to perform classification of patient clinical status based on this. And the network and regional tau measures are higher in tau positive than in tau negative participants. Subjects with higher tau regional measures tend to have higher tau network measures.

3.3. Individual network measurements—In AD, MCI, and CU groups

Group comparison for each tau network measurements including global efficiency, global strength, and limbic strength was performed controlling for age and gender (Figure 4). Tau composite SUVRs and entorhinal SUVRs were also compared among the three groups (Figure 4). All tau network measures showed significant difference among the 3 groups ($p < 2.0e-19$, ANCOVA), as well as the pairwise separation ($p < 0.001$). Of note, all network measures (i.e., global efficiency, global strength) increase from CU to AD. The tau SUVR measures also showed similar group separation ($p < 8.0e-20$, ANCOVA) and pairwise separation ($p < 0.001$). In Table 2, we see the Cohen's f based on ANCOVA analysis for the 3 group with age and gender as the covariate. All network and regional measures show a large effect

(Cohen's $f > 0.4$) for separation among AD, MCI and CU. Tau global strength demonstrated largest Cohen's f (0.69, Table 2), followed by tau composite SUVR (0.62). Table 3 shows the effect size for the pairwise analyses CU versus MCI and AD versus MCI. The tau measures with largest effect size in analysis between MCI and CU is tau global strength and entorhinal SUVR (Cohen's $f = 0.34$) followed by tau limbic strength (Cohen's $f = 0.33$). The tau measures with largest effect size in analysis between MCI and AD is tau global strength (Cohen's $f = 0.57$) followed by and tau composite SUVR (Cohen's $f = 0.51$). Network (global strength and limbic strength) and regional measures have clinically relevant effect sizes for both pairwise group comparisons (AD vs. MCI groups and MCI vs. CU groups). Global efficiency has lower effect sizes in CU/MCI pairwise assessment. As expected, the best regional measurement for effect size analyses of CU and MCI is entorhinal and the best regional SUVR measurement for effect size analyses of MCI vs. AD is tau composite SUVR.

3.4. Relationship of tau PET (network and regional) to memory

The association of tau measures with AVLT-LTM in full group as well as within CU subjects separately was shown in

TABLE 2 Effect sizes, Cohen's f , from either FTP PET network measures or regional measure volumes for the for ancova of the three groups (AD, MCI, CU).

	AD/MCI/CU
Tau global efficiency	0.52 (0.40, 0.624)*
Tau global strength	0.69 (0.575, 0.80)
Tau limbic strength	0.60 (0.49, 0.71)
Tau composite SUVR	0.62 (0.50, 0.73)
Tau entorhinal SUVR	0.52 (0.41, 0.63)

Cohen's f , 95% confidence intervals are shown and covariates included in the analysis were age and gender. *Cohen's f (95% confidence intervals).

TABLE 3 Effect sizes, Cohen's f , from either FTP PET network measures or regional measure volumes for the for pair wise analysis of the three groups (AD, MCI, CU).

	AD/CU	AD/MCI	MCI/CU
Tau global efficiency	0.62 (0.49, 0.76)*	0.47(0.29, 0.64)	0.22 (0.11, 0.33)
Tau global strength	0.82 (0.67, 0.96)	0.57 (0.39, 0.75)	0.34(0.23, 0.45)
Tau limbic strength	0.74 (0.60, 0.88)	0.46 (0.29, 0.64)	0.33 (0.22, 0.44)
Tau composite SUVR	0.70 (0.56, 0.84)	0.51 (0.33, 0.68)	0.31 (0.20, 0.42)
Tau entorhinal SUVR	0.64 (0.50, 0.77)	0.34 (0.17, 0.51)	0.34 (0.23, 0.45)

Cohen's f , 95% confidence intervals are shown and covariates included in the analysis were age and gender. *Cohen's f (95% confidence intervals).

Figure 5. In the full group where AVLT-LTM has values covering the full range, all tau measures were significantly associated with AVLT-LTM (**Figure 5A**). The correlation between global efficiency and AVLT-LTM is significantly stronger than the correlation between AVLT-LTM and tau composite ($p < 0.04$). The correlations between both global strength and limbic strength and AVLT-LTM are also significantly stronger than the correlation between AVLT-LTM and regional measurements ($p < 0.04$). In CU, only two tau network measures were significantly associated with AVLT-LTM, (tau global efficiency: $r_s = -0.24$, $p = 0.002$, tau global strength: $r_s = -0.16$, $p = 0.04$, **Figure 5B**), other tau measures did not show a significant association. The results were similar when restricted to amyloid positive participants only. All tau measures were significantly associated with AVLT-LTM ($p < 0.05$) in amyloid positive participants across the clinical spectrum. In amyloid positive CU participants, only limbic strength is correlated with AVLT-LTM ($r_s = -0.37$, $p = 0.03$), global efficiency and strength as well as tau SUVR measures was not significantly associated with AVLT-LTM.

3.5. Staging with tau PET measures

We show the staging based on using global efficiency, and limbic strength as seen in **Figure 6A**. There are two thresholds for limbic strength, first a threshold = 14.46 to divide participants into stage 1–2 and 3–4 and then a threshold = 9.867 to divide stage 1–2 into stage 1 and stage 2. A threshold of global efficiency = 0.901 was found to divide participants into stage 3 and stage 4. The average tau PET image for each of the 4 stages defined based on tau network measures was illustrated in **Figure 6B**. The spatial

pattern of tau burden across the 4 stages resembles the pattern described by Braak staging with tau accumulation starting from the medial temporal lobe and spreading to the isocortical regions. It appears that on average in the early stages there might be some tau starting not only in medial temporal lobe but also precuneus.

4. Discussion

In this paper we introduce individualized tau network measurements using graph theory that allows the assessment of tangle burden across the entire brain. Global strength, global efficiency, and limbic strength in the tau networks are higher in AD subjects (AD > MCI > CU). Global strength, global efficiency and limbic strength had similar effect sizes compared to traditional regional SUVR measures of tau burden. The network measures and regional measures showed similar discrimination between AD and CU. As an example of the discriminative ability between AD and CU of the tau measures, limbic strength demonstrated an AUC (95% confidence interval) = 0.90 [0.83, 0.97], specificity = 0.88, sensitivity = 0.83. In general, both tau network measures and the regional SUVR measures correlated with memory score, while only the network measures (global efficiency, global strength were significantly correlated with memory in the CU group). These findings suggest our proposed tau network analysis approach can be a useful technique in providing an overall assessment of tau burden with strong statistical power in differentiating clinical AD stages and predicting cognitive performance. Further investigation with larger cohorts may be able to determine whether network-based measurements had superior statistical power for group separation. We also demonstrated our approach to be more sensitive to detecting the relationship between tangle burden and cognitive decline prior to clinical symptoms. Visually, the stages determined based on global efficiency and limbic strength also resemble the general pattern of tau progression as defined based on Braak staging. Fifty three percent of the CU in stage 3 and 4 are A β positive, 47% of the CU in stage 3 and 4 are APOE4 carriers. 90% of the CU in stage 3 and stage 4 are tau positive. It should be noted that the gold standard for Braak staging should be based on neuropathological assessment while tau PET can partially replicate that although it should be interpreted with caution (Lowe et al., 2020; Soleimani-Meigooni et al., 2020). Numerous studies have shown deviations from typical Braak staging based spatial patterns and individual variability exists in where tau starts in the cortex and how it progresses (Braak et al., 2011; Franzmeier et al., 2020; Sanchez et al., 2021; Vogel et al., 2021). The goal of performing staging based on network measure in this study is mainly to demonstrate its similarity with the Braak based staging system. Further study is warranted to examine the validity and performance of this staging system using both cross-sectional and longitudinal data.

In the association analysis between tau measures and AVLT-LTM, excluding amyloid negative participants did not substantially change the observed association. All tau measures were associated with AVLT-LTM across the clinical spectrum and only certain tau network measures can detect an association in the CU

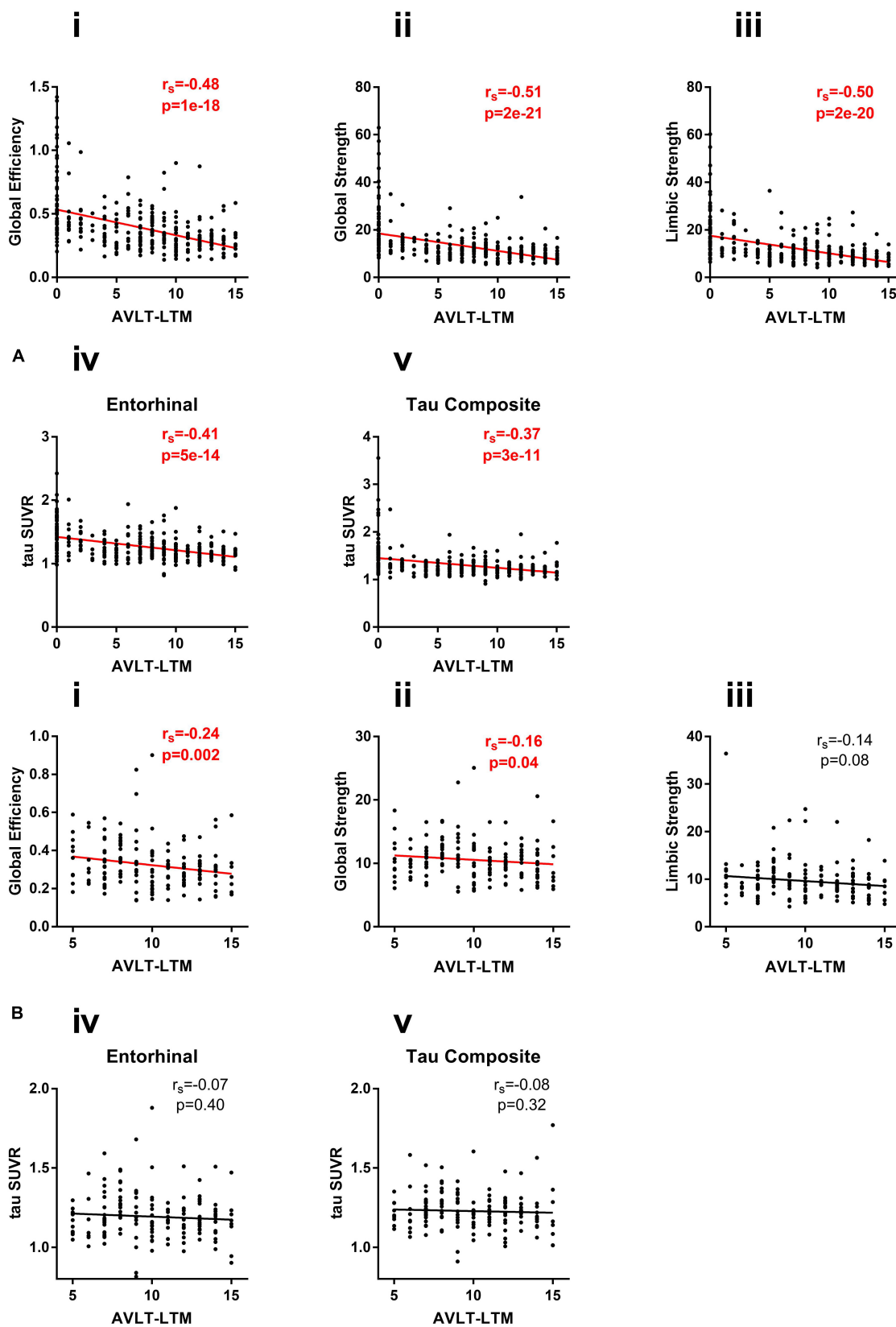
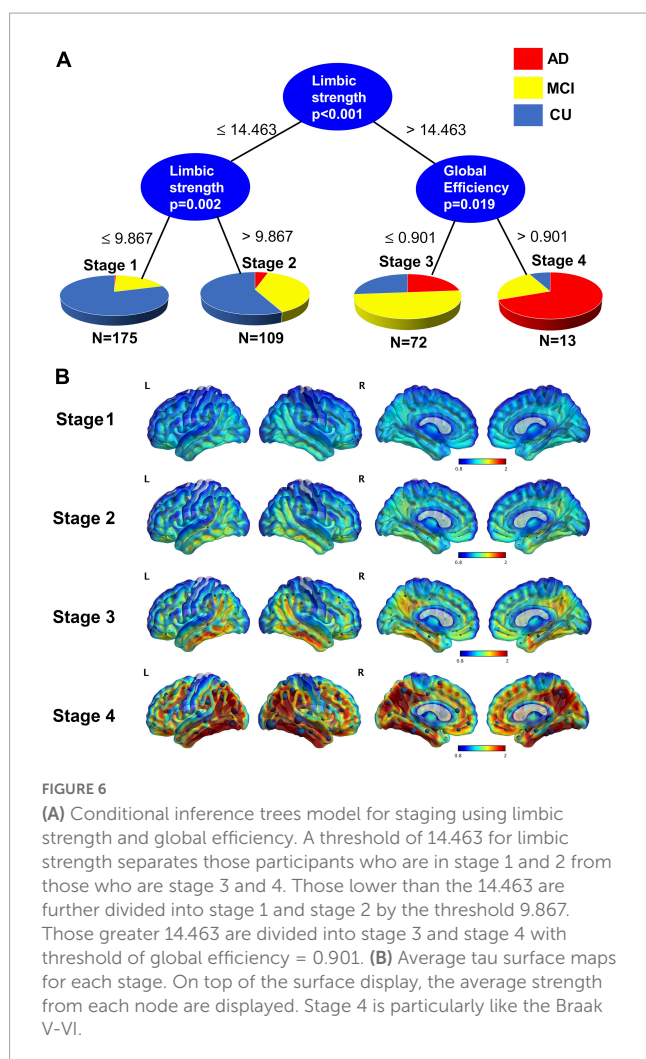


FIGURE 5 (A) Correlation of network measures (i) global efficiency, (ii) global strength, and (iii) limbic strength, and regional measures (iv) entorhinal SUVR, and (v) tau composite SUVR with AVLT-LTM in all subjects (CU/MCI/AD). (B) Correlation of network measures (i) global efficiency, (ii) global strength, and (iii) limbic strength and regional measures (iv) entorhinal SUVR, and (v) tau composite SUVR with AVLT-LTM in CU subjects.



group. While focusing on amyloid positive participants allows us to investigate the spectrum of patients fitting the typical pathological profile of AD it also results in reduced sample size and preventing us from examine the very early phase of the disease. The subtle difference of which network measure were associated with AVLT-LTM in the CU group depending on the amyloid status may be a results of sample size differences or underlying differences in tau distribution pattern that require further investigation.

We primarily examined AVLT-LTM which is more sensitive to earlier cognitive changes. AVLT-LTM is a sensitive measure to detect memory decline including at early stages when participants are still considered cognitively normal (Caselli et al., 2009). We also examined correlation with Clinical Dementia Rating Scale-Sum of Boxes (CDR-SB), Mini Mental State examination (MMSE), AVLT-total, and AVLT-STM. The results were consistent with our findings with AVLT-LTM. All cognitive measures were significantly correlated with conventional tau SUVR measures as well as network based measures, while the relationship tend to be stronger for network measures. Also, in CU participants, only network-based measures were found to be significantly correlated with cognitive measurements.

In our proposed technique to derive individualized tau networks, the nodes were defined based on average gray matter maps in MNI template space with each node centered within each individual AAL region, and each node is represented by a cube in the imaging space. We also investigated the influence of tau PET analysis pipelines and choice of nodes for the construction of the individualized tau networks. These results were summarized in the [Supplementary material](#). We found our approach to be generally robust and not sensitive to the detailed variation in the implementation of the network model such as the size of the cube, the number of nodes, and template space vs. individual space analysis. These findings support the generalized application of our proposed approach to different tau analysis pipelines without losing its power to detect tau changes and its association with cognition. We did not compare in this manuscript the individualized network with a group-based network like tau covariance since the group based networks and individual based networks serve different purposes and the goal of this manuscript was to demonstrate the utility of our individual based networks which allows the assessment of tau burden and its spatial distribution at individual level. Group based networks only examine the spatial pattern of tau distribution. A comparison of the two approaches is beyond the scope of our current study although would be interesting for future study.

In network analysis pruning of edges or weights is a commonly performed task. To examine the sensitivity of our tau network analysis approach to such pruning, we included two different implementation of individualized tau network with one using 86 FreeSurfer defined nodes including both cortical and subcortical regions and another one focusing on the cortical regions only given the off-target binding in subcortical regions (Baker et al., 2019). The results are largely similar in that the network metrics' ability to differentiate clinical groups and correlating with memory scores are not affected by the two implementations.

Although tau PET tracers are designed to target tau fibril tangles, tau PET images nevertheless carry structural information due to the difference in non-specific tracer retention among different tissue types, e.g., gray vs. white matter. To better understand whether the network measures derived from tau PET images are primarily driven by specific tau binding rather than non-specific signal which would resemble more of structural MR data, we applied the same approach to construct individual level gray matter and white matter networks based on tissue density map derived from T1w-MRI, and subsequently evaluated these T1w-MRI derived network measures in their ability to differentiate AD diagnostic groups and their association with cognition ([Supplementary Tables 5–7](#)). It was determined that the T1w-MRI derived network measures had far less power in differentiate the clinical groups ([Supplementary Table 5](#)). We also found that the T1w-MRI derived network measures had weaker or no association with cognition and sometimes in the opposite direction ([Supplementary Tables 6, 7](#)). These observations suggest that our proposed tau network measures are driven more by the specific tau-binding related signals which further strengthens their utility in assessing tau pathologies.

In summary, we proposed and evaluated a novel approach to construct individualized tau network and compute graph-theoretical measures of the network. We found these measures to differentiate clinical stages and have stronger associations with cognition compared to regional measures, particularly in CU. In addition, this method can be applied to other tauopathies and subtypes of AD that show differing patterns of tau deposition. Additional investigation is needed to relate these tau network measures with other AD related changes such as amyloid and neurodegeneration as well as determine its power in track longitudinal changes of tangle burden. This method can be further extended to a longitudinal network to measure longitudinal tau spread. For future work we will also examine the ability of using network measures to determine tau positivity. Further investigation is also warranted to determine whether these subtle tau changes identified by network analysis can be detected in other tauopathies.

Data availability statement

The original contributions presented in this study are included in the article/[Supplementary material](#), further inquiries can be directed to the corresponding author.

Ethics statement

The studies involving human participants were reviewed and approved by the Alzheimer's Disease Neuroimaging Initiative. The patients/participants provided their written informed consent to participate in this study.

Author contributions

HP: methodology, conceptualization, investigation and analysis and writing. VG: investigation and writing original draft. DG, KC, and ER: investigation and reviewing and editing. RB and VD: data management. YS: methodology, conceptualization, investigation, supervision, and writing—review and editing. All authors contributed to the article and approved the submitted version.

Funding

Data collection and sharing for this project was funded by the Alzheimer's Disease Neuroimaging Initiative (ADNI) (National Institutes of Health Grant U01 AG024904) and DOD ADNI (Department of Defense award number W81XWH-12-2-0012). ADNI is funded by the National Institute on Aging, the National Institute of Biomedical Imaging and Bioengineering, and through generous contributions from the following: AbbVie, Alzheimer's Association; Alzheimer's Drug Discovery Foundation; Araclon Biotech; BioClinica, Inc.; Biogen; Bristol-Myers Squibb Company; CereSpir, Inc.; Cogstate; Eisai Inc.; Elan Pharmaceuticals, Inc.; Eli Lilly and Company; EuroImmun; F. Hoffmann-La Roche Ltd and

its affiliated company Genentech, Inc.; Fujirebio; GE Healthcare; IXICO Ltd.; Janssen Alzheimer Immunotherapy Research & Development, LLC.; Johnson & Johnson Pharmaceutical Research & Development LLC.; Lumosity; Lundbeck; Merck & Co., Inc.; MesoScale Diagnostics, LLC.; NeuroRx Research; Neurotrack Technologies; Novartis Pharmaceuticals Corporation; Pfizer Inc.; Piramal Imaging; Servier; Takeda Pharmaceutical Company; and Transition Therapeutics. The Canadian Institutes of Health Research is providing funds to support ADNI clinical sites in Canada. Private sector contributions are facilitated by the Foundation for the National Institutes of Health (www.fnih.org). The grantee organization is the Northern California Institute for Research and Education, and this study was coordinated by the Alzheimer's Therapeutic Research Institute at the University of Southern California. ADNI data are disseminated by the Laboratory for Neuro Imaging at the University of Southern California. Research reported in this publication was supported by the National Institute on Aging of the National Institutes of Health under Award Numbers U19AG024904, R01AG069453, R01AG031581, P30AG072980, P30AG019610, and RF1AG073424 and Grant No. CTR057001 from Arizona Department of Health Services to Arizona Alzheimer's Research Center.

Acknowledgments

Data used in preparation of this article were obtained from the Alzheimer's Disease Neuroimaging Initiative (ADNI) database (adni.loni.usc.edu). As such, the investigators within the ADNI contributed to the design and implementation of ADNI and/or provided data but did not participate in analysis or writing of this report. A complete listing of ADNI investigators can be found at: http://adni.loni.usc.edu/wp-content/uploads/how_to_apply/ADNI_Acknowledgement_List.pdf.

Conflict of interest

The authors declare that the research was conducted in the absence of any commercial or financial relationships that could be construed as a potential conflict of interest.

Publisher's note

All claims expressed in this article are solely those of the authors and do not necessarily represent those of their affiliated organizations, or those of the publisher, the editors and the reviewers. Any product that may be evaluated in this article, or claim that may be made by its manufacturer, is not guaranteed or endorsed by the publisher.

Supplementary material

The Supplementary Material for this article can be found online at: <https://www.frontiersin.org/articles/10.3389/fnins.2023.1089134/full#supplementary-material>

References

- Albert, M. S. (2011). Changes in cognition. *Neurobiol. Aging* 32(Suppl. 1), S58–S63. doi: 10.1016/j.neurobiolaging.2011.09.010
- Arlt, S., Buchert, R., Spies, L., Eichenlaub, M., Lehmebeck, J. T., and Jahn, H. (2013). Association between fully automated MRI-based volumetry of different brain regions and neuropsychological test performance in patients with amnesic mild cognitive impairment and Alzheimer's disease. *Eur. Arch. Psychiatry Clin. Neurosci.* 263, 335–344. doi: 10.1007/s00406-012-0350-7
- Arnemann, K. L., Stober, F., Narayan, S., Rabinovici, G. D., and Jagust, W. J. (2018). Metabolic brain networks in aging and preclinical Alzheimer's disease. *Neuroimage Clin.* 17, 987–999. doi: 10.1016/j.nicl.2017.12.037
- Baker, S. L., Harrison, T. M., Maass, A., La Joie, R., and Jagust, W. (2019). Effect of off-target binding on (18)F-Flortaucipir variability in healthy controls across the lifespan. *J. Nucl. Med.* 60, 1444–1451. doi: 10.2967/jnumed.118.224113
- Braak, H., Alafuzoff, I., Arzberger, T., Kretschmar, H., and Del Tredici, K. (2006). Staging of Alzheimer disease-associated neurofibrillary pathology using paraffin sections and immunocytochemistry. *Acta Neuropathol.* 112, 389–404. doi: 10.1007/s00401-006-0127-z
- Braak, H., and Braak, E. (1991). Neuropathological staging of Alzheimer-related changes. *Acta Neuropathol.* 82, 239–259. doi: 10.1007/bf00308809
- Braak, H., and Braak, E. (1995). Staging of Alzheimer's disease-related neurofibrillary changes. *Neurobiol. Aging* 16, 271–278. doi: 10.1016/0197-4580(95)00021-6
- Braak, H., Thal, D. R., Ghebremedhin, E., and Del Tredici, K. (2011). Stages of the pathological process in Alzheimer disease: Age categories from 1 to 100 years. *J. Neuropathol. Exp. Neurol.* 70, 960–969. doi: 10.1097/NEN.0b013e318232a379
- Braun, U., Plichta, M. M., Esslinger, C., Sauer, C., Haddad, L., Grimm, O., et al. (2012). Test-retest reliability of resting-state connectivity network characteristics using fMRI and graph theoretical measures. *Neuroimage* 59, 1404–1412. doi: 10.1016/j.neuroimage.2011.08.044
- Caselli, R. J., Dueck, A. C., Osborne, D., Sabbagh, M. N., Connor, D. J., Ahern, G. L., et al. (2009). Longitudinal modeling of age-related memory decline and the APOE epsilon4 effect. *N. Engl. J. Med.* 361, 255–263. doi: 10.1056/NEJMoa0809437
- Chien, D. T., Bahri, S., Szardenings, A. K., Walsh, J. C., Mu, F., Su, M. Y., et al. (2013). Early clinical PET imaging results with the novel PHF-tau radioligand [F-18]-T807. *J. Alzheimer Dis.* 34, 457–468. doi: 10.3233/JAD-122059
- Dani, M., Brooks, D. J., and Edison, P. (2016). Tau imaging in neurodegenerative diseases. *Eur. J. Nucl. Med. Mol. Imaging* 43, 1139–1150. doi: 10.1007/s00259-015-3231-2
- Dyer, R. J. (2009). GeneticStudio: A suite of programs for spatial analysis of genetic-marker data. *Mol. Ecol. Resour.* 9, 110–113. doi: 10.1111/j.1755-0998.2008.02384.x
- Dyer, R. J., and Nason, J. D. (2004). Population graphs: The graph theoretic shape of genetic structure. *Mol. Ecol.* 13, 1713–1727. doi: 10.1111/j.1365-294X.2004.02177.x
- Dyer, R. J., Nason, J. D., and Garrick, R. C. (2010). Landscape modelling of gene flow: Improved power using conditional genetic distance derived from the topology of population networks. *Mol. Ecol.* 19, 3746–3759. doi: 10.1111/j.1365-294X.2010.04748.x
- Excoffier, L., Smouse, P. E., and Quattro, J. M. (1992). Analysis of molecular variance inferred from metric distances among DNA haplotypes: Application to human mitochondrial DNA restriction data. *Genetics* 131, 479–491. doi: 10.1093/genetics/131.2.479
- Farahani, F. V., Karwowski, W., and Lighthall, N. R. (2019). Application of graph theory for identifying connectivity patterns in human brain networks: A systematic review. *Front. Neurosci.* 13:585. doi: 10.3389/fnins.2019.00585
- Fleisher, A. S., Chen, K., Liu, X., Roontiva, A., Thiyyagura, P., Ayutyanont, N., et al. (2011). Using positron emission tomography and florbetapir F18 to image cortical amyloid in patients with mild cognitive impairment or dementia due to Alzheimer disease. *Arch. Neurol.* 68, 1404–1411. doi: 10.1001/archneurol.2011.150
- Fornito, A., Zalesky, A., and Bullmore, E. T. (2010). Network scaling effects in graph analytic studies of human resting-state fMRI data. *Front. Syst. Neurosci.* 4:22. doi: 10.3389/fnsys.2010.00022
- Franzmeier, N., Dewenter, A., Frontzkowski, L., Dichgans, M., Rubinski, A., Neitzel, J., et al. (2020). Patient-centered connectivity-based prediction of tau pathology spread in Alzheimer's disease. *Sci. Adv.* 6:eabd1327. doi: 10.1126/sciadv.abd1327
- Garroway, C. J., Bowman, J., Carr, D., and Wilson, P. J. (2008). Applications of graph theory to landscape genetics. *Evol. Appl.* 1, 620–630. doi: 10.1111/j.1752-4571.2008.00047.x
- He, Y., Chen, Z., and Evans, A. (2008). Structural insights into aberrant topological patterns of large-scale cortical networks in Alzheimer's disease. *J. Neurosci.* 28, 4756–4766. doi: 10.1523/JNEUROSCI.0141-08.2008
- He, Y., Chen, Z. J., and Evans, A. C. (2007). Small-world anatomical networks in the human brain revealed by cortical thickness from MRI. *Cereb. Cortex* 17, 2407–2419. doi: 10.1093/cercor/bhl149
- Hojjati, S. H., Ebrahimzadeh, A., and Babajani-Feremi, A. (2019). Identification of the early stage of Alzheimer's disease using structural MRI and resting-state fMRI. *Front. Neurol.* 10:904. doi: 10.3389/fneur.2019.00904
- Huang, S., Li, J., Sun, L., Ye, J., Fleisher, A., Wu, T., et al. (2010). Learning brain connectivity of Alzheimer's disease using sparse inverse covariance estimation. *Neuroimage* 50, 935–949. doi: 10.1016/j.neuroimage.2009.12.120
- Ivnik, R. J., Malec, J. F., Smith, G. E., Tangalos, E. G., Petersen, R. C., Kokmen, E., et al. (1992). Mayo's older Americans normative studies: Updated AVLT norms for ages 56 to 97. *Clin. Neuropsychol.* 6, 83–104. doi: 10.1080/13854049208401880
- Jack, C. R. Jr., Bennett, D. A., Blennow, K., Carrillo, M. C., Dunn, B., Haeberlein, S. B., et al. (2018). NIA-AA research framework: toward a biological definition of Alzheimer's disease. *Alzheimers Dement.* 14, 535–562. doi: 10.1016/j.jalz.2018.02.018
- Jack, C. R. Jr., Knopman, D. S., Jagust, W. J., Shaw, L. M., Aisen, P. S., Weiner, M. W., et al. (2010). Hypothetical model of dynamic biomarkers of the Alzheimer's pathological cascade. *Lancet Neurol.* 9, 119–128. doi: 10.1016/S1474-4422(09)70299-6
- Jack, C. R. Jr., Wiste, H. J., Weigand, S. D., Therneau, T. M., Lowe, V. J., Knopman, D. S., et al. (2017b). Defining imaging biomarker cut points for brain aging and Alzheimer's disease. *Alzheimers Dement.* 13, 205–216. doi: 10.1016/j.jalz.2016.08.005
- Jack, C. R. Jr., Wiste, H. J., Weigand, S. D., Therneau, T. M., Knopman, D. S., Lowe, V., et al. (2017a). Age-specific and sex-specific prevalence of cerebral β -amyloidosis, tauopathy, and neurodegeneration in cognitively unimpaired individuals aged 50–95 years: A cross-sectional study. *Lancet Neurol.* 16, 435–444.
- Johnson, K. A., Schultz, A., Betensky, R. A., Becker, J. A., Sepulcre, J., Rentz, D., et al. (2016). Tau positron emission tomographic imaging in aging and early Alzheimer disease. *Ann. Neurol.* 79, 110–119. doi: 10.1002/ana.24546
- Kim, C. M., Montal, V., Diez, I., Orwig, W., Alzheimer's Disease Neuroimaging Initiative [ADNI], and Sepulcre, J. (2021). Network interdigitations of tau and amyloid-beta deposits define cognitive levels in aging. *Hum. Brain Mapp.* 42, 2990–3004. doi: 10.1002/hbm.25350
- Lowe, V. J., Lundt, E. S., Albertson, S. M., Min, H. K., Fang, P., Przybelski, S. A., et al. (2020). Tau-positron emission tomography correlates with neuropathology findings. *Alzheimers Dement.* 16, 561–571. doi: 10.1016/j.jalz.2019.09.079
- Maass, A., Landau, S., Baker, S. L., Horng, A., Lockhart, S. N., La Joie, R., et al. (2017). Comparison of multiple tau-PET measures as biomarkers in aging and Alzheimer's disease. *Neuroimage* 157, 448–463. doi: 10.1016/j.neuroimage.2017.05.058
- Manel, S., and Holderegger, R. (2013). Ten years of landscape genetics. *Trends Ecol. Evol.* 28, 614–621. doi: 10.1016/j.tree.2013.05.012
- Morris, J. C., Storandt, M., Miller, J. P., McKeel, D. W., Price, J. L., Rubin, E. H., et al. (2001). Mild cognitive impairment represents early-stage Alzheimer disease. *Arch. Neurol.* 58, 397–405.
- Pereira, J. B., Strandberg, T. O., Palmqvist, S., Volpe, G., van Westen, D., Westman, E., et al. (2018). Amyloid network topology characterizes the progression of Alzheimer's disease during the predementia stages. *Cereb. Cortex* 28, 340–349. doi: 10.1093/cercor/bhx294
- Rodger, Y. S., Greenbaum, G., Silver, M., Bar-David, S., and Winters, G. (2018). Detecting hierarchical levels of connectivity in a population of *Acacia tortilis* at the northern edge of the species' global distribution: Combining classical population genetics and network analyses. *PLoS One* 13:e0194901. doi: 10.1371/journal.pone.0194901
- Rubinow, M., and Sporns, O. (2010). Complex network measures of brain connectivity: Uses and interpretations. *Neuroimage* 52, 1059–1069. doi: 10.1016/j.neuroimage.2009.10.003
- Sanchez, J. S., Becker, J. A., Jacobs, H. I. L., Hanseeuw, B. J., Jiang, S., Schultz, A. P., et al. (2021). The cortical origin and initial spread of medial temporal tauopathy in Alzheimer's disease assessed with positron emission tomography. *Sci. Transl. Med.* 13:eabc0655. doi: 10.1126/scitranslmed.abc0655
- Savary, P., Foltete, J.-C., Moal, H., Vuidel, G., and Garnier, S. (2021a). graph4lg: A package for constructing and analysing graphs for landscape genetics in R. *Methods Ecol. Evol.* 12, 539–547. doi: 10.1111/2041-210X.13530
- Savary, P., Foltete, J. C., Moal, H., Vuidel, G., and Garnier, S. (2021b). Analysing landscape effects on dispersal networks and gene flow with genetic graphs. *Mol. Ecol. Resour.* 21, 1167–1185. doi: 10.1111/1755-0998.13333
- Scholl, M., Lockhart, S. N., Schonhaut, D. R., O'Neil, J. P., Janabi, M., Ossenkoppele, R., et al. (2016). PET imaging of tau deposition in the aging human brain. *Neuron* 89, 971–982. doi: 10.1016/j.neuron.2016.01.028
- Schwarz, A. J., Shcherbinin, S., Sliker, L. J., Risacher, S. L., Charil, A., Izrarry, M. C., et al. (2018). Topographic staging of tau positron emission tomography images. *Alzheimers Dement.* 10, 221–231. doi: 10.1016/j.dadm.2018.01.006

- Schwarz, A. J., Yu, P., Miller, B. B., Shcherbinin, S., Dickson, J., Navitsky, M., et al. (2016). Regional profiles of the candidate tau PET ligand 18F-AV-1451 recapitulate key features of Braak histopathological stages. *Brain* 139, 1539–1550. doi: 10.1093/brain/aww023
- Sepulcre, J., Grothe, M. J., d'Oleire Uquillas, F., Ortiz-Teran, L., Diez, I., Yang, H. S., et al. (2018). Neurogenetic contributions to amyloid beta and tau spreading in the human cortex. *Nat. Med.* 24, 1910–1918. doi: 10.1038/s41591-018-0206-4
- Sepulcre, J., Sabuncu, M. R., Becker, A., Sperling, R., and Johnson, K. A. (2013). In vivo characterization of the early states of the amyloid-beta network. *Brain* 136, 2239–2252. doi: 10.1093/brain/awt146
- Shirk, A. J., Landguth, E. L., and Cushman, S. A. (2018). A comparison of regression methods for model selection in individual-based landscape genetic analysis. *Mol. Ecol. Resour.* 18, 55–67. doi: 10.1111/1755-0998.12709
- Soleimani-Meigooni, D. N., Iaccarino, L., La Joie, R., Baker, S., Bourakova, V., Boxer, A. L., et al. (2020). 18F-flortaucipir PET to autopsy comparisons in Alzheimer's disease and other neurodegenerative diseases. *Brain* 143, 3477–3494. doi: 10.1093/brain/awaa276
- Tijms, B. M., Moller, C., Vrenken, H., Wink, A. M., de Haan, W., van der Flier, W. M., et al. (2013). Single-subject grey matter graphs in Alzheimer's disease. *PLoS One* 8:e58921. doi: 10.1371/journal.pone.0058921
- Tijms, B. M., Series, P., Willshaw, D. J., and Lawrie, S. M. (2012). Similarity-based extraction of individual networks from gray matter MRI scans. *Cereb. Cortex* 22, 1530–1541. doi: 10.1093/cercor/bhr221
- Tijms, B. M., Ten Kate, M., Gouw, A. A., Borta, A., Verfaillie, S., Teunissen, C. E., et al. (2018). Gray matter networks and clinical progression in subjects with predementia Alzheimer's disease. *Neurobiol. Aging* 61, 75–81. doi: 10.1016/j.neurobiolaging.2017.09.011
- Tzourio-Mazoyer, N., Landeau, B., Papathanassiou, D., Crivello, F., Etard, O., Delcroix, N., et al. (2002). Automated anatomical labeling of activations in SPM using a macroscopic anatomical parcellation of the MNI MRI single-subject brain. *Neuroimage* 15, 273–289. doi: 10.1006/nimg.2001.0978
- Veronese, M., Moro, L., Arcolin, M., Dipasquale, O., Rizzo, G., Expert, P., et al. (2019). Covariance statistics and network analysis of brain PET imaging studies. *Sci. Rep.* 9:2496. doi: 10.1038/s41598-019-39005-8
- Vogel, J. W., Young, A. L., Oxtoby, N. P., Smith, R., Ossenkuppe, R., Strandberg, O. T., et al. (2021). Four distinct trajectories of tau deposition identified in Alzheimer's disease. *Nat. Med.* 27, 871–881. doi: 10.1038/s41591-021-01309-6
- Wang, H., Jin, X., Zhang, Y., and Wang, J. (2016). Single-subject morphological brain networks: Connectivity mapping, topological characterization and test-retest reliability. *Brain Behav.* 6:e00448. doi: 10.1002/brb3.448
- Wang, J., Zuo, X., and He, Y. (2010). Graph-based network analysis of resting-state functional MRI. *Front. Syst. Neurosci.* 4:16. doi: 10.3389/fnsys.2010.00016
- Wang, J. H., Zuo, X. N., Gohel, S., Milham, M. P., Biswal, B. B., and He, Y. (2011). Graph theoretical analysis of functional brain networks: Test-retest evaluation on short- and long-term resting-state functional MRI data. *PLoS One* 6:e21976. doi: 10.1371/journal.pone.0021976
- Wang, M., Jiang, J., Yan, Z., Alberts, I., Ge, J., Zhang, H., et al. (2020). Individual brain metabolic connectome indicator based on kullback-leibler divergence similarity estimation predicts progression from mild cognitive impairment to Alzheimer's dementia. *Eur. J. Nucl. Med. Mol. Imaging* 47, 2753–2764. doi: 10.1007/s00259-020-04814-x
- Xia, M., Wang, J., and He, Y. (2013). BrainNet viewer: A network visualization tool for human brain connectomics. *PLoS One* 8:e68910. doi: 10.1371/journal.pone.0068910
- Yu, B., Sun, H., Ma, H., Peng, M., Kong, F., Meng, F., et al. (2013). Aberrant whole-brain functional connectivity and intelligence structure in children with primary nocturnal enuresis. *PLoS One* 8:e51924. doi: 10.1371/journal.pone.0051924